

Circuit Electromechanics with a Non-Metallized Nanobeam

M. Pernpeintner,^{1,2,3,a)} T. Faust,⁴ F. Hocke,^{1,2,3} J. P. Kotthaus,⁴ E. M. Weig,^{4,5} H. Huebl,^{1,2,b)} and R. Gross^{1,2,3}

¹⁾ Walther-Meißner-Institut, Bayerische Akademie der Wissenschaften, D-85748 Garching, Germany

²⁾ Nanosystems Initiative Munich, Schellingstraße 4, D-80799 München, Germany

³⁾ Physik-Department, Technische Universität München, D-85748 Garching, Germany

⁴⁾ Center for NanoScience (CeNS) and Fakultät für Physik, Ludwig-Maximilians-Universität, D-80799 München, Germany

⁵⁾ Department of Physics, University of Konstanz, D-78457 Konstanz, Germany

(Dated: 29 July 2014)

We have realized a nano-electromechanical hybrid system consisting of a silicon nitride beam dielectrically coupled to a superconducting microwave resonator. We characterize the sample by making use of the Duffing nonlinearity of the strongly driven beam. In particular, we calibrate the amplitude spectrum of the mechanical motion and determine the electromechanical vacuum coupling. A high quality factor of 480,000 at a resonance frequency of 14 MHz is achieved at 0.5 K. The experimentally determined electromechanical vacuum coupling of 11.5 mHz is quantitatively compared with finite element based model calculations.

In the field of cavity optomechanics, micro- or nanoscale mechanical resonators are coupled to an optical cavity allowing to transfer information from the mechanical to the optical domain and vice versa^{1–6}. For example, such optomechanical systems have recently been used to observe interference effects like optomechanically induced transparency⁸ or to cool mechanical resonators to their ground state⁷. Moreover, they have been e.g. proposed for quantum information processing⁹ or for the detection of gravitational waves¹⁰. To increase the performance of such systems, high mechanical quality factors and high resonance frequencies are desirable, which are provided e.g. by strongly pre-stressed Si₃N₄ thin films^{11–13}. Analogous to optical cavities, electrical circuits can be coupled to nanomechanical resonators giving rise to the field of cavity nano-electromechanics^{14–19}. Typically, a metallized mechanical resonator is capacitively coupled to a superconducting microwave resonator enabling e.g. ground state cooling¹⁷ or the control of microwave signals¹⁹. In order to enable a further increase of quality factors it is beneficial to avoid any additional dissipation due to the metallization of the mechanical resonator^{20–22}. To this end, the dielectric coupling of non-metallized Si₃N₄ nanoresonators has been established as an alternative transduction and control scheme for high-Q nano-electromechanical systems in recent years^{12,23}. Here, the displacement is detected dielectrically via a microwave cavity's resonance frequency which immediately enables cavity electromechanics²⁴. For the temperature range between 10 and 300 K, conventional copper microstrip cavities have been successfully employed. Millikelvin temperature operation can be achieved by integrating a pure, i.e. non-metallized, nanomechanical beams into a superconducting microwave circuit. This approach is promising for the realization of high quality factors of both the

mechanical and the microwave resonator.

In this letter we demonstrate such an integrated nano-electromechanical system where a pure insulating silicon nitride nanobeam is coupled to a superconducting coplanar waveguide microwave resonator. We calibrate the mechanical amplitude of the beam and use its nonlinear Duffing response to obtain the electromechanical coupling (cf. ref. 25). We find a vacuum coupling of $g_0/2\pi = 11.5$ mHz which is corroborated quantitatively by finite element modelling of the system.

Our nano-electromechanical device consists of a doubly-clamped, highly tensile-stressed Si₃N₄ nanobeam which is dielectrically coupled to a $\lambda/2$ superconducting niobium microwave resonator. The beam is located between the niobium centerline and ground plane with a gap of 150 nm between beam and electrodes, as shown in Fig. 1a-c. The sample is fabricated on a single-crystalline silicon wafer coated with 400 nm of thermal oxide and 100 nm of highly tensile-stressed LPCVD silicon nitride (Si₃N₄). First, a $l = 20$ μ m long and $w = 170$ nm wide nanobeam as well as supporting clamping rectangles are defined using e-beam lithography and covered with aluminum serving as an etch mask. Subsequently, the unprotected silicon nitride and approximately 100 nm of SiO₂ are removed by an anisotropic SF₆ reactive ion etching (RIE) step. In this way, we align the lower surface of the beam (i.e. the SiO₂-Si₃N₄ interface) approximately with the upper surface of the subsequently deposited niobium film (cf. schematic displayed in Fig. 4a). With a second e-beam lithography step followed by aluminum sputtering, we define a small rectangularly-shaped protective cover for the Si₃N₄ beam and its vicinity. Then, a 100 nm thick niobium film is deposited by magnetron sputtering. Subsequently, the microwave resonator and its input and output lines are patterned by a third e-beam lithography and a second RIE step. The resist and the aluminum coating are removed with acetone, potassium hydroxide and Piranha (i.e. a mixture of hydrogen peroxide and sulphuric acid). Finally, we release the silicon

^{a)} Electronic mail: matthias.pernpeintner@wmi.badw.de

^{b)} Electronic mail: hans.huebl@wmi.badw.de

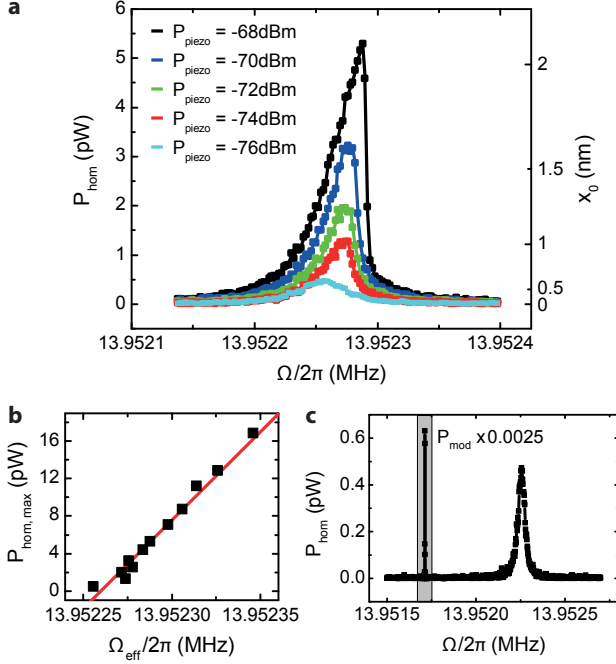


FIG. 3. **a.** Homodyne power spectrum (left axis) resp. mechanical amplitude spectrum (right axis) of the nanobeam for varying external drive power. The amplitude scale (on the right) is based on the amplitude calibration described in the main text. **b.** Maximum homodyne power as a function of the effective resonance frequency (the so-called backbone curve). **c.** Homodyne power spectrum for low external drive ($P_{\text{piezo}} = -76$ dBm) using a frequency-modulated cavity drive tone. The sideband peak at $\Omega_{\text{mod}}/2\pi = 13.9517$ MHz is scaled by a factor of 0.0025. Comparing the heights of both sideband peaks allows to determine the vacuum coupling g_0 .

lator is given by the implicit equation³⁰

$$\left[\Gamma_m^2 + 4 \left(\Omega - \Omega_m - \frac{3}{8} \frac{\alpha}{\Omega_m} x_0^2 \right)^2 \right] x_0^2 = \frac{F^2}{m_{\text{eff}}^2 \Omega_m^2}. \quad (4)$$

Thus, for increasing drive power the maximum of the amplitude spectrum, $x_{0,\text{max}}$, shifts to higher frequencies Ω_{eff} , as illustrated in Fig. 3a. This dependence is described by the backbone curve³⁰

$$x_{0,\text{max}}^2 = \frac{8}{3} \frac{\Omega_m}{\alpha} (\Omega_{\text{eff}} - \Omega_m). \quad (5)$$

As a consequence, we can relate the amplitude x_0 of the beam to spectral information, which is straightforwardly accessible.

To determine the coupling between the microwave cavity and the nanobeam, we analyze the quadrature response of the superconducting microwave cavity. To this end, we calibrate this response with a known frequency modulation Ω_{mod} of the microwave carrier frequency ω_d (refs. 19,26) as shown in Fig. 3c (highlighted in gray). Hereby, we can relate the detected power of the homodyne signal P_{hom} to the well-known frequency modula-

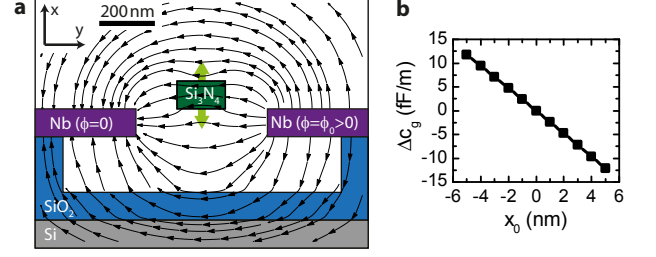


FIG. 4. **a.** Two-dimensional static COMSOL model to simulate the electromechanical coupling. The black arrows indicate the electric field strength and direction, resulting from an electrostatic potential difference ϕ_0 between the niobium electrodes. The light green arrow illustrates the dynamic displacement of the nanobeam (not to scale). **b.** Calculated capacitance change per length, $\Delta c_g(x_0) \equiv c_g(x_0) - c_g(0)$, as a function of the beam displacement x_0 .

tion depth, or in other words, we can determine the transfer function $K(\Omega_{\text{mod}})$. We choose $\Omega_{\text{mod}} \approx \Omega_m$ and therefore assume $K(\Omega_{\text{mod}}) \approx K(\Omega_m)$ ^{19,26}.

Using Eq. (1), the backbone curve Eq. (5) reads

$$P_{\text{hom,max}} = \frac{8}{3} \frac{\Omega_m}{\alpha} \frac{K(\Omega_m) G^2}{\Omega_m^2} (\Omega_{\text{eff}} - \Omega_m) \quad (6)$$

where $P_{\text{hom,max}} \equiv P_{\text{hom}}(\Omega_{\text{eff}})$ denotes the down-converted signal power at the effective resonance frequency Ω_{eff} , that is, at the maximum of the $P_{\text{hom}}(\Omega)$ curve. Thus, measuring the homodyne power spectrum of the beam as a function of the external driving force imposed by the piezoactuator and plotting $P_{\text{hom,max}}$ versus Ω_{eff} , as shown in Fig. 3b, allows to extract the coupling constant G . With $K(\Omega_m) = 2.4 \times 10^{-3} \text{ W}$, $E = 160 \text{ GPa}$ (ref. 1), $\sigma = 830 \text{ MPa}$ (ref. 1), $\rho = 2600 \text{ kg/m}^3$ (ref. 24) and $m_{\text{eff}} = 0.43 \text{ pg}$, we obtain $G/2\pi = 312 \text{ Hz/nm}$. Thus, the electromechanical vacuum coupling is $g_0/2\pi = G/2\pi \cdot x_{\text{zpf}} = 11.5 \text{ mHz}$ (ref. 26) with the zero-point fluctuation of the beam $x_{\text{zpf}} = \sqrt{\hbar/2m_{\text{eff}}\Omega_m} = 37 \text{ fm}$ (ref. 33). Compared to similar nano-electromechanical hybrid systems with metallized beams (see e.g. ref. 19), the coupling is about two orders of magnitude smaller, as it solely relies on the dielectric interaction between nanobeam and niobium electrodes.

To understand the electro-mechanical coupling mechanism in more detail and to estimate the coupling constant a priori, we use a COMSOL 2D model representing the cross-sectional sample area perpendicular to the longitudinal nanobeam direction (see Fig. 4a, cf. ref. 12). Hereby, we calculate the capacitance per length, c_g , between center line and ground plane for various (static) displacements x_0 of the nanobeam. The result is plotted in Fig. 4b. We find a capacitance change per displacement of $\partial c_g / \partial x_0 = 2.4 \text{ (fF/m)/nm}$. Due to the vibrating nanobeam the total capacitance C of the microwave resonator has two contributions: a static part C_0 and a displacement-dependent oscillating part $C_g(x_0) = c_g(x_0)l_{\text{eff}}$, where $l_{\text{eff}} = 0.613l$ is the effective length of the

beam²⁸.

The resonance frequency of a superconducting $\lambda/2$ coplanar waveguide resonator is given by $\omega_c = 1/\sqrt{LC}$, where L denotes the inductance of the resonator³⁴. Thus, assuming $C_g/C_0 \ll 1$, the resonance frequency can be rewritten as

$$\omega_c(x_0) \approx \omega_0 \left(1 - \frac{C_g(x_0)}{2C_0} \right), \quad (7)$$

where we have introduced the resonance frequency of the microwave cavity for an undisplaced beam, $\omega_0 = 1/\sqrt{LC_0}$. With the line impedance Z_0 , we obtain the coupling constant

$$G = -\frac{\partial \omega_c}{\partial x_0} = \frac{Z_0 \omega_0^2}{\pi} \frac{\partial C_g}{\partial x_0}. \quad (8)$$

Using the numerically obtained value $\partial C_g/\partial x_0 = 2.4$ (fF/m)/nm, the measured resonance frequency of the microwave cavity $\omega_0/2\pi = 5.67$ GHz and its designed impedance value $Z_0 = 70 \Omega$, we obtain $G/2\pi = 132$ Hz/nm or $g_0/2\pi = 4.8$ mHz. Although the simulation uses only an approximation of the real sample geometry, this is in good agreement with the experimentally determined value, demonstrating that the applied modeling is useful for an a-priori estimation of the nano-electromechanical coupling of a given sample geometry.

In conclusion, we have fabricated and characterized a nano-electromechanical hybrid system consisting of a superconducting microwave resonator and a non-metallized nanomechanical beam. On decreasing the temperature, for a beam with a resonance frequency of about 14 MHz we observe an increase of the mechanical quality factor from 40,000 at room temperature³⁵ to 480,000 at 550 mK. For strong external driving forces we observe the transition from the linear to the Duffing regime and use this to quantify the mechanical displacement amplitude of the beam. Fitting the peak values of the measured homodyne power spectra allows us to precisely determine the mechanical amplitude. This method is complementary to the usually employed calibration via thermal motion^{26,36} and especially useful for systems where the Brownian motion is not straightforwardly detectable. Moreover, the precise knowledge of the motional amplitude allows us to derive the electromechanical coupling g_0 . For our device, we find $g_0/2\pi = 11.5$ mHz, which is corroborated by numerical modeling of the device.

This work opens the path for further experimental studies of mechanical losses in silicon nitride at millikelvin temperatures, extending previous work on the damping mechanisms in Si_3N_4 nanomechanical beams^{1,37}. Moreover, the concept of dielectrically coupling a pure Si_3N_4 nanobeam to a high- Q microwave resonator is promising especially for sensing devices, e.g. for the detection of single molecules, which require high frequency resolution and thus low damping constants.

Financial support by the Deutsche Forschungsgemeinschaft via Project No. Ko 416/18 is gratefully acknowledged.

- ¹T. J. Kippenberg, H. Rokhsari, T. Carmon, A. Scherer, and K. J. Vahala, *Physical Review Letters* **95**, 033901 (2005).
- ²S. Gigan, H. R. Bhm, M. Paternostro, F. Blaser, G. Langer, J. B. Hertzberg, K. C. Schwab, D. Buerle, M. Aspelmeyer, and A. Zeilinger, *Nature* **444**, 67 (2006).
- ³O. Arcizet, P.-F. Cohadon, T. Briant, M. Pinard, and A. Heidmann, *Nature* **444**, 71 (2006).
- ⁴D. Kleckner and D. Bouwmeester, *Nature* **444**, 75 (2006).
- ⁵J. D. Thompson, B. M. Zwickl, A. M. Jayich, F. Marquardt, S. M. Girvin, and J. G. E. Harris, *Nature* **452**, 72 (2008).
- ⁶M. Aspelmeyer, T. J. Kippenberg, and F. Marquardt, eds., *Cavity Optomechanics – Nano- and Micromechanical Resonators Interacting with Light* (Springer, 2014).
- ⁷J. Chan, T. P. M. Alegre, A. H. Safavi-Naeini, J. T. Hill, A. Krause, S. Gröblacher, M. Aspelmeyer, and O. Painter, *Nature* **478**, 89 (2011).
- ⁸S. Weis, R. Riviere, S. Delglise, E. Gavartin, O. Arcizet, A. Schliesser, and T. J. Kippenberg, *Science* **330**, 1520 (2010).
- ⁹K. Stannigel, P. Komar, S. J. M. Habraken, S. D. Bennett, M. D. Lukin, P. Zoller, and P. Rabl, *Physical Review Letters* **109**, 013603 (2012).
- ¹⁰R. Kaltenbaek, G. Hechenblaikner, N. Kiesel, O. Romero-Isart, K. C. Schwab, U. Johann, and M. Aspelmeyer, *Experimental Astronomy* **34**, 123 (2012).
- ¹¹S. S. Verbridge, J. M. Parpia, R. B. Reichenbach, L. M. Bel-lan, and H. G. Craighead, *Journal of Applied Physics* **99**, 124304 (2006).
- ¹²Q. P. Unterreithmeier, E. M. Weig, and J. P. Kotthaus, *Nature* **458**, 1001 (2009).
- ¹³P.-L. Yu, T. P. Purdy, and C. A. Regal, *Physical Review Letters* **108**, 083603 (2012).
- ¹⁴C. A. Regal, J. D. Teufel, and K. W. Lehnert, *Nature Physics* **4**, 555 (2008).
- ¹⁵A. D. O'Connell, M. Hofheinz, M. Ansmann, R. C. Bialczak, M. Lenander, E. Lucero, M. Neeley, D. Sank, H. Wang, M. Weides, J. Wenner, J. M. Martinis, and A. N. Cleland, *Nature* **464**, 697 (2010).
- ¹⁶T. Rocheleau, T. Ndukum, C. Macklin, J. B. Hertzberg, A. A. Clerk, and K. C. Schwab, *Nature* **463**, 72 (2010).
- ¹⁷J. D. Teufel, D. Li, M. S. Allman, K. Cicak, A. J. Sirois, J. D. Whittaker, and R. W. Simmonds, *Nature* **471**, 204 (2011).
- ¹⁸J. D. Teufel, T. Donner, D. Li, J. W. Harlow, M. S. Allman, K. Cicak, A. J. Sirois, J. D. Whittaker, K. W. Lehnert, and R. W. Simmonds, *Nature* **475**, 359 (2011).
- ¹⁹X. Zhou, F. Hocke, A. Schliesser, A. Marx, H. Huebl, R. Gross, and T. J. Kippenberg, *Nature Physics* **9**, 179 (2013).
- ²⁰F. W. Beil, R. H. Blick, A. Wixforth, W. Wegscheider, D. Schuh, and M. Bichler, *EPL (Europhysics Letters)* **76**, 1207 (2006).
- ²¹E. Collin, J. Kofler, S. Lakhroufi, S. Pairis, Y. M. Bunkov, and H. Godfrin, *Journal of Applied Physics* **107**, 114905 (2010).
- ²²K. Das, G. Sosale, and S. Vengallatore, *Nanotechnology* **23**, 505703 (2012).
- ²³J. Rieger, T. Faust, M. J. Seitner, J. P. Kotthaus, and E. M. Weig, *Applied Physics Letters* **101**, 103110 (2012).
- ²⁴T. Faust, P. Krenn, S. Manus, J. P. Kotthaus, and E. M. Weig, *Nature Communications* **3**, 728 (2012).
- ²⁵F. Hocke, M. Pernpeintner, X. Zhou, A. Schliesser, T. J. Kippenberg, H. Huebl, and R. Gross, arXiv:1407.6867 [cond-mat.mes-hall].
- ²⁶M. L. Gorodetsky, A. Schliesser, G. Anetsberger, S. Deleglise, and T. J. Kippenberg, *Optics Express* **18**, 23236 (2010).
- ²⁷F. Hocke, *Microwave circuit-electromechanics in a nano-mechanical hybrid system*, Ph.D. thesis, Technische Universität München, Walther-Meißner-Institut für Tieftemperaturforschung (2013).
- ²⁸see Supplemental Material.
- ²⁹S. Timoshenko, *Vibration Problems in Engineering* (D. Van Nostrand Company, Inc., 1937).
- ³⁰A. H. Nayfeh and D. T. Mook, *Nonlinear Oscillations* (John Wiley & Sons, New York, 1979).

- ³¹Q. P. Unterreithmeier, S. Manus, and J. P. Kotthaus, *Applied Physics Letters* **94**, 263104 (2009).
- ¹Q. P. Unterreithmeier, T. Faust, and J. P. Kotthaus, *Physical Review Letters* **105**, 027205 (2010).
- ³³T. J. Kippenberg and K. J. Vahala, *Science* **321**, 1172 (2008).
- ³⁴M. Göppl, A. Fragner, M. Baur, R. Bianchetti, S. Filipp, J. M. Fink, P. J. Leek, G. Puebla, L. Steffen, and A. Wallraff, *Journal of Applied Physics* **104**, 113904 (2008).

- ³⁵The room temperature quality factor of the nanobeam has been determined by optical interferometry.
- ³⁶B. D. Hauer, C. Doolin, K. S. D. Beach, and J. P. Davis, *Annals of Physics* **339**, 181 (2013).
- ³⁷T. Faust, J. Rieger, M. J. Seitner, J. P. Kotthaus, and E. M. Weig, *Physical Review B* **89**, 100102 (2014).

Supplemental Material: Circuit Electromechanics with a Non-Metallized Nanobeam

A. EFFECTIVE MASS OF THE BEAM

According to the Supplementary Information of ref. S1, the total energy of the oscillating beam is given by

$$U = \frac{1}{2} \rho w t \Omega_m^2 \int_{-l/2}^{l/2} dz x_0^2(z), \quad (\text{S1})$$

where $x_0(z)$ is the z -dependent displacement of the beam, ρ and Ω_m are the density of the beam resp. its resonance frequency, and w , t and l denote width, thickness and length of the beam.

Following Euler-Bernoulli beam theory^{S2,S3}, the displacement $x_0(z)$ of the fundamental mode of the presented tensile-stressed doubly-clamped beam is given by

$$x_0(z) = a_1 e^{\alpha z} + a_2 e^{-\alpha z} + a_3 \sin(\beta z) + a_4 \cos(\beta z) \quad (\text{S2})$$

with the numerically calculated coefficients $\alpha = 2.50 \times 10^6 \text{ m}^{-1}$, $\beta = 1.63 \times 10^5 \text{ m}^{-1}$, $a_1 = a_2 = 9.04 \times 10^{-13} a_4$ and $a_3 = -3.30 \times 10^{-13} a_4$.

With that, the integral in (S1) can be solved numerically:

$$\int_{-l/2}^{l/2} dz x_0^2(z) = 0.480 l a_4^2$$

We define the effective mass m_{eff} of the beam by

$$U = \frac{1}{2} m_{\text{eff}} \Omega_m^2 x_{0,c}^2 \quad (\text{S3})$$

where $x_{0,c} := x_0(z=0)$ is the displacement of the center of the beam.

Comparing Eqs. (S1) and (S3), we get

$$m_{\text{eff}} = \frac{\rho w t}{x_{0,c}^2} \int_{-l/2}^{l/2} dz x_0^2(z) = 0.480 \rho w t l = 0.43 \text{ pg}$$

B. EFFECTIVE LENGTH OF THE NANOBEAM

As described in the main text, a static 2D COMSOL model is employed to calculate the effect of the beam displacement on the capacitance between center line and ground plane of the microwave resonator. Considering that the displacement x_0 is a function of the position z along the beam, the capacitance variation δC_g induced by a displacement $x_0(z)$ is given by

$$\delta C_g = \frac{\partial c_g}{\partial x} \int_{-l/2}^{l/2} dz x_0(z)$$

In linear approximation, we write

$$\frac{\partial C_g}{\partial x} \approx \frac{\delta C_g}{x_{0,c}} = \frac{\partial c_g}{\partial x} \int_{-l/2}^{l/2} dz \frac{x_0(z)}{x_{0,c}}$$

As above, the integral can be solved numerically using (S2):

$$\int_{-l/2}^{l/2} dz \frac{x_0(z)}{x_{0,c}} = 0.613 l$$

Thus, we have

$$\frac{\partial C_g}{\partial x} = \frac{\partial c_g}{\partial x} \cdot l_{\text{eff}}$$

where $l_{\text{eff}} = 0.613 l$ is the effective length of the beam.

ADDITIONAL REFERENCES

- [S1]Q. P. Unterreithmeier, T. Faust, and J. P. Kotthaus, Physical Review Letters **105**, 027205 (2010).
- [S2]F. Hocke, M. Pernpeintner, X. Zhou, A. Schliesser, T. J. Kippenberg, H. Huebl, and R. Gross, arXiv:1407.6867 [cond-mat.mes-hall].
- [S3]S. Timoshenko, Vibration Problems in Engineering (D. Van Nostrand Company, Inc., 1937).